Pure Appl. Chem., Vol. 77, No. 9, pp. 1607–1616, 2005.
DOI: 10.1351/pac200577091607

Modeling the active site structures of vanadate-dependent peroxidases and vanadate-inhibited phosphatases*

Dieter Rehder‡, Martin Ebel, Cornelia Wikete, Gabriella Santoni, and Jessica Gätjens

Institut für Anorganische und Angewandte Chemie, Universität Hamburg, D20146 Hamburg, Germany

Abstract: The active center of vanadate-dependent peroxidases (VPOs) is represented by vanadate covalently attached to a histidine, with vanadium in a trigonal–bipyramidal environment. Protein phosphatases and kinases are inhibited by the phosphate analog vanadate [$V^{V}O_2(OH)_2^-$ and $V^{IV}O(OH)_3^-$], which can be related to the coordination of vanadium to histidine or a hydroxide function as provided by tyrosinate or serinate. The vanadium centers in these proteins have been modeled by employing chiral ONO ligands. The penta-coordinated chiral complexes [$VO(OMe)(L^1)$] (H_2L^1 = substituted diethanolamine) are distorted trigonal–bipyramidal with the methoxy group and the amine-N in the axial positions. These structural models of VPO also mimic the sulfide-oxidation activity of the peroxidases. The complexes [$VO(H_2O)L^3$] (H_2L^3 = Schiff-base ligands based on salicylaldehyde derivatives (*o*-vanillin; 2-hydroxy-naphthylaldehyde) and L- or D,L-tyrosine, or D,L-serine are tetragonal–pyramidal; the OH functions of the amino acid moieties are not directly coordinated to vanadium; they are involved, however, in complex hydrogen-bonding networks. The oxo/peroxo anion $[VO(O_2)(L^2)_2]^{3-}$ (H_2L^2 = 2,5-dipicolinic acid) contains a slightly asymmetrically bonded O_2^{2-}, featuring structural characteristics of the peroxo/hydroperoxo intermediates of the peroxidases. XD structure results are reported for the following complexes: *R*,*S*- and *R*,*R*-[$VO(OMe)(L^1)$], $K_3[VO(O_2)(L^2)_2]\cdot 4.5H_2O$, the Tyr derivatives L-[$VO(H_2O)L^3$]·MeOH and D,L-[$VO(H_2O)L^3$]·H_2O, and the Ser derivative D,L-[$VO(H_2O)L^3$]·$2H_2O$.

Keywords: Haloperoxidases; phosphatases; vanadate; vanadium complexes; amino acids.

INTRODUCTION

Vanadate-dependent haloperoxidases (VPOs) catalyze the 2-electron oxidation, by peroxide, of halides to hypohalous acid, and of (prochiral) sulfides to (chiral) sulfoxides [1], eqs. 1a and 2. The enzymatic formation of hypohalous acid is followed by the nonenzymatically halogenation of organic substrates, eq. 1b. The enzymes have been isolated from marine algae, from a lichen and a fungus. Structural characterization is available for the peroxidases obtained from the brown marine alga *Ascophyllum nodosum* [2], the red algae *Corallina oficinalis* and *C. pilulifera* [3], and the fungus *Curvularia inaequalis* [4a], including a variety of mutants [4b,c] and the peroxo form [5] of the latter. All of these enzymes contain

*Paper based on a presentation at the 4th International Symposium on Chemistry and Biological Chemistry of Vanadium, Szeged, Hungary, 3–5 September 2004. Other presentations are published in this issue, pp. 1497–1640.

‡Corresponding author

the same cofactor, viz. vanadate covalently attached to histidine-Nε of the protein; Fig. 1, **a**. Vanadium is in a trigonal–bipyramidal environment with the doubly bonded oxo group in the plane and His in one of the axial positions. This is also the dominating feature in certain *acid* phosphatases inhibited by vanadate [6], Fig. 1, **b**. Under physiological conditions, vanadate is available as vanadate(V) [$H_2VO_4^- \equiv VO_2(OH)_2^-$] and, in the nanomolar concentration range, vanadate(IV) [$VO(OH)_3^-$]. Both forms may be considered phosphate analogues. Vanadate-inhibited *alkaline* phosphatases contain serinate [7] or cysteinate [8] at the binding site, Fig. 1, **c**. Serine is also close to (and in H-bonding contact with) the active center of the VPOs. This similarity between peroxidases and phosphatases is not restricted to the vanadate center, but extends, in the case of peroxidases and acid phosphatases, to the amino acid sequence at the active centers [4b,9] and to motifs in the tertiary structure, suggesting convergent evolution or a common evolutionary origin. Furthermore, ViPs have some haloperoxidase activity [10], while the apoperoxidases have been shown to exhibit some phosphatase activity [9,11].

$$Hal^- + H_2O_2 + H^+ \rightarrow HOHal + H_2O \quad (1a)$$

$$HOHal + RH \rightarrow RHal + H_2O \quad (1b)$$

$$SRR' + H_2O_2 \rightarrow O{=}SRR' + H_2O \quad (2)$$

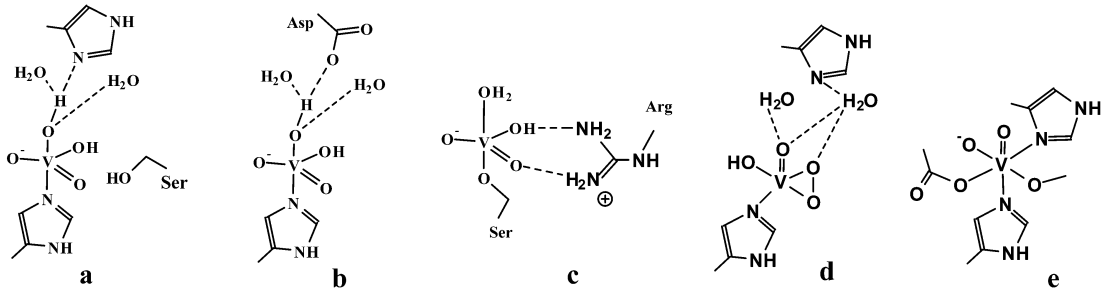

Fig. 1 The active centers of (VPOs) [**a:** native form, **d:** peroxo form, **e:** proposed reduced form (inactive)], and vanadate-inhibited rat acid phosphatase (**b**) and alkaline phosphatase from *E. coli* (**c**).

For the catalytic cycle, a peroxo (and hydroperoxo) intermediate [12] as well as a hypobromito intermediate [13] have been proposed (Fig. 2). In the peroxo form, which has been structurally characterized [5], a square–pyramidal geometry prevails (Fig. 1, **d**), with the symmetrically coordinated peroxo ligand in the plane and the oxo group in the apex. Reduction of the *A. nodosum* enzyme to the vanadyl (VO^{2+}) forms leads to its inactivation and rearrangements in the coordination sphere, including coordination of a second N-donor [14]; Fig. 1, **e**.

In the present study, we report on oxovanadium(IV) and –(V) complexes with an overall NO_4 donor set in a (distorted) trigonal–bipyramidal or square–pyramidal environment, with the nitrogen function provided by an amine- or imine-N. These complexes model structure features of the active sites of peroxidases and the vanadate-inhibited phosphatases (ViPs). Vanadate is well known to inhibit phosphate-metabolizing enzymes such as phosphatases, kinases, and ribonucleases [15]. In several specific cases, stimulation may also occur; an example is phosphoglycerate mutase [16]. It has been proposed that these interactions are due to coordination of vanadate to histidine, hydroxide of tyrosine, serine, or threonine at the active site of the phosphatase. This view has been corroborated by structural evidence on an alkaline phosphatase from *Escherichia coli* [7], a bovine phosphotyrosyl phosphatase [8] and a rat acid phosphatase [6b]. In the case of cysteine in the active site, redox and non-redox inactivation by vanadates may occur [17]. We complement our structural models by a peroxo complex, i.e., a model for an active intermediate in oxo transfer to a substrate, and by catalytically conducted enantioselective sulfide oxidation and thus a model reaction for the function of the enzyme.

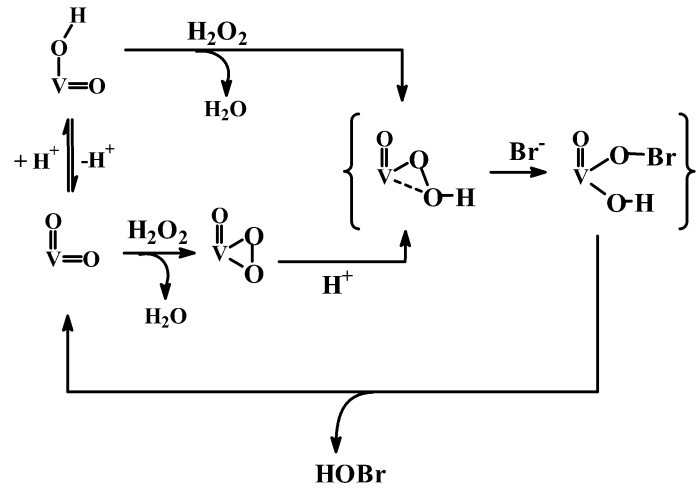

Fig. 2 Possible catalytic cycle for the oxo transfer to bromide by bromoperoxidase from *A. nodosum.* Other 2e$^-$ oxidation products than HOBr can form, such as Br_2 or Br_3^-.

COMPLEXES WITH AMINO-BIS(ETHANOLS)

The ligands H_2L^1 are prepared from styrene oxide and the respective amine 1,2-($\mathbf{L^{1(2)}}$) or 1,3- ($\mathbf{L^{1(1)}}$) by ring opening (Scheme 1) and purified by flash chromatography on silica gel; see ref. [18] for analogous reactions. Reaction of H_2L^1 with VO(*i*Pr)$_3$ in methanol yields the complexes [VO(OMe)L^1] (**1** and **2**; Scheme 1) in the *R*,*S* (**1**) and *R*,*R* configurations (**2**), respectively. Characteristic IR data are collated in Table 1.

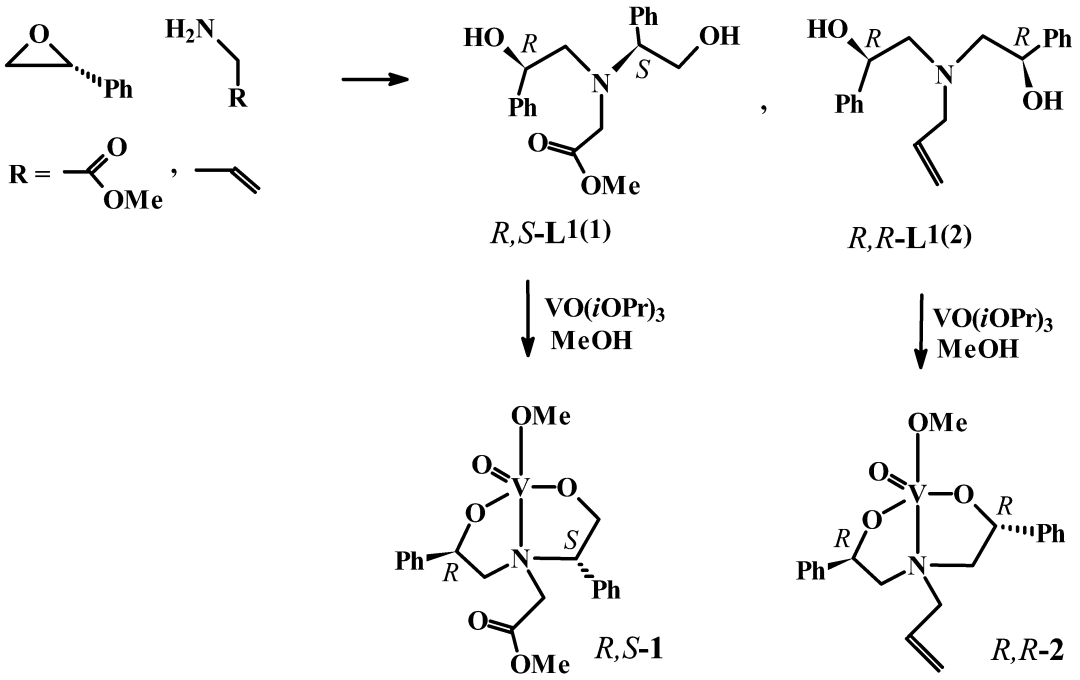

Scheme 1

Table 1 Selected IR data (cm^{-1}) for **1–5**.

	ν(V=O)	ν(R_2N–CH_2) or νN=CH)	ν(C–O)	$\nu_{ass}(CO_2)$	$\nu_{sym}(CO_2)$
1	967	2812	1027		
2	970	2887	1046		
3[a]	971			1629	1378
4a	1005, 977sh	1621, 1608			
4b	984	1626, 1606			
5	988	1623, 1605		1685	1384

[a]ν_{ass}(O–O) = 952 cm^{-1}.

Both complexes crystallize in the monoclinic space group *P*2(1). Selected bonding parameters are compiled in Table 2, ORTEP plots are shown in Fig. 3. The τ values [18], 0.73 for **1**, 0.75 and 0.77 for the two independent molecules in the asymmetric unit of **2**, indicate slight distortions from the trigonal–bipyramidal (τ = 1) toward the square–pyramidal arrangement (τ = 0), which compares to other complexes with related ligands [19] and clearly differs from the otherwise commonly observed square–pyramidal geometry of five-coordinated oxovanadium complexes. Compounds **1** and **2** thus are structural mimicks of the active center of the peroxidase and vanadate-inhibited acid phosphatase (acid ViP), **a** and **b** in Fig. 1. The chirality provided by the active site amino acids of the enzyme may be considered to be modeled by the chiral centers in the ligand periphery of the complexes. In addition, the compounds model a functional feature of the peroxidases, viz. their enantioselective sulfideperoxidase activity (eq. 2). We have investigated the model system benzylphenylsulfide/cumylhydroperoxide/vanadium catalyst (molar ratio 1/1/0.1; temperature –20 °C). The best results with respect to selectivity (sulfoxide vs. sulfone), yield, reaction time, and ee (37 % of the *R*,*R* enantiomer) have been obtained with the in situ system $VO(OiPr)_3$/*R*,*R*-$\mathbf{L^{1(3)}}$. The results, graphically presented in Fig. 4, compare to those obtained with related [19] and other vanadium-based catalyst systems [20]. Considerably higher ee have been reported for systems based on Schiff-base ligands that derive from substituted salicylaldehyde and chiral amino-monoalcohols [21]. The fairly low ee for our complexes possibly reflects flexibility and thus the presence of several isomers in solution, as evidenced by the ^{51}V NMR chemical shifts, $\delta(^{51}V)$ = –452 and –470 ppm (ratio of integral intensities 2:1) for **1**, and –418, –446, and –455 ppm (1.0:0.25:0.15) for **2**.

Table 2 Selected bond lengths (Å) and angles (°) for complexes **1–5**[a].

[VO($\mathbf{L^{1(1)}}$)], **1**	[VO($\mathbf{L^{1(2)}}$)], **2**[b]	[$VO(O_2)(\mathbf{L^2})_2$]$^{3-}$, **3**[b]	[VO($\mathbf{L^{3(2)}}$)], **4b**	[VO($\mathbf{L^{3(3)}}$)], **5**
V-O6 1.590(5)	V-O1 1.6037(15)	V-O1 1.596(3)	V-O1 1.5944(16)	V-O1 1.596(3)
V-O5 1.749(4)	V-O4 1.7849(15)	V-O2 2.039(3)	V-O2 1.9773(16)	V-O2 1.972(3)
V-O1 1.807(5)	V-O2 1.8002(13)	V-O6 2.175(3)	V-O4 1.9043(15)	V-O4 1.894(3)
V-N1 2.562(5)	V-N1 2.3526(17)	V-O10/11 1.851/1.883(3)	V-O5 2.0077(16)	V-O5 1.979(3)
		V-N1/N2 2.135/2.127(3)	V-N 2.0341(18)	V-N 2.022(3)
		O10-O11 1.394(4)		
N1-V-O5 167.8(2)	O4-V-N1 168.60(6)	O1-V-O6 168.48(12)	O2-V-O4 141.97(7)	O2-V-O4 141.83(12)

(*continues on next page*)

Table 2 (*Continued*).

[VO($\mathbf{L}^{1(1)}$)], **1**	[VO($\mathbf{L}^{1(2)}$)], **2**[b]	[VO(O_2)($\mathbf{L}^{2}$)$_2$]$^{3-}$, **3**[b]	[VO($\mathbf{L}^{3(2)}$)], **4b**	[VO($\mathbf{L}^{3(3)}$)], **5**
O1-V-O2 124.3(2)	O2-V-O3 123.72(7)	N1-V-N2 150.69(12)	O5-V-N 147.61(8)	O5-V-N 149.11(14)
O1-V-O6 109.3(3)	O2-V-O1 114.16(7)	N1-V-O10 78.58(12)	O4-V-N 87.79(7)	O4-V-N 87.65(12)
		O2-V-O10 151.06(12)	O2-V-N 78.63(7)	O2-V-N 78.91(12
		O10-V-O11 43.68(11)		

[a]See Schemes 1 and 2 for ligand abbreviations.
[b]For one of the two independent molecules.

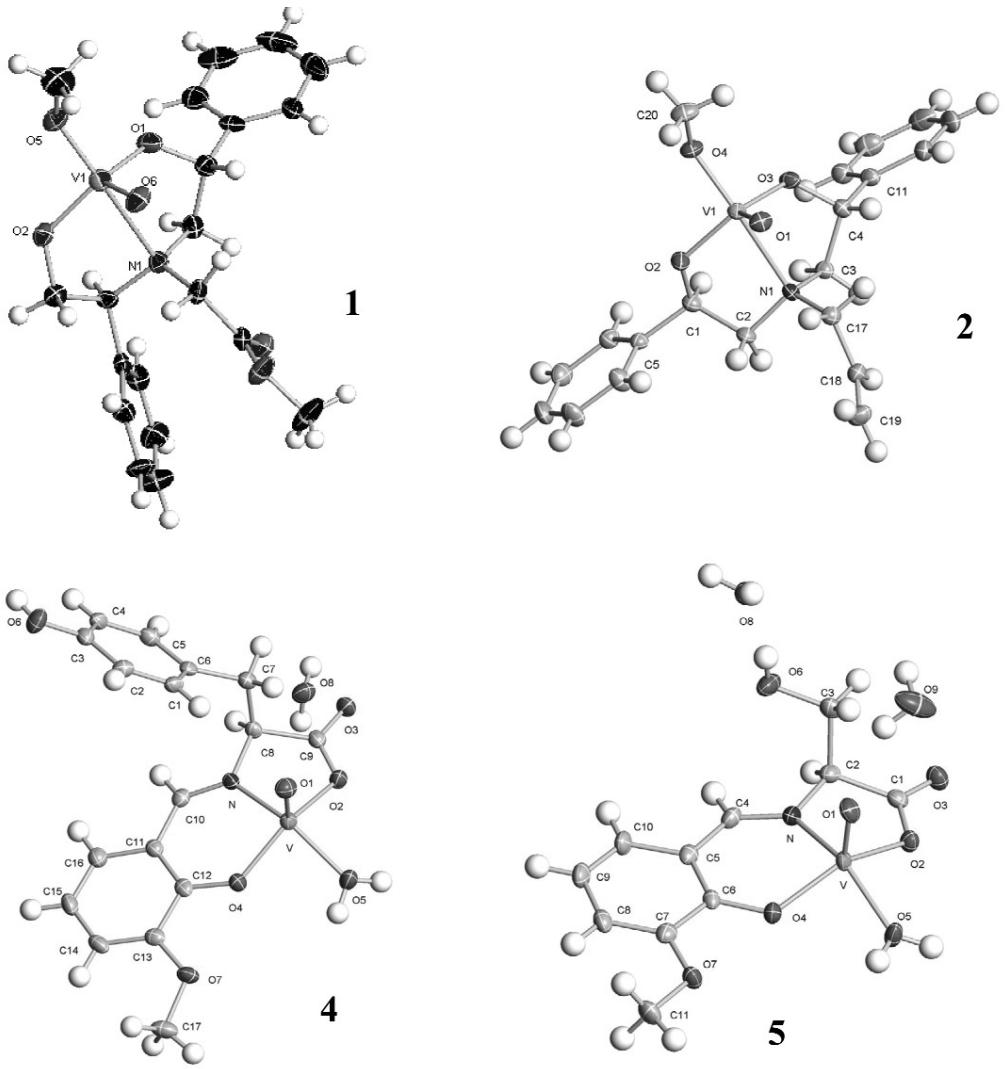

Fig. 3 ORTEP plots of complexes **1**, **2**, **4b**·H_2O, and **5**·2H_2O.

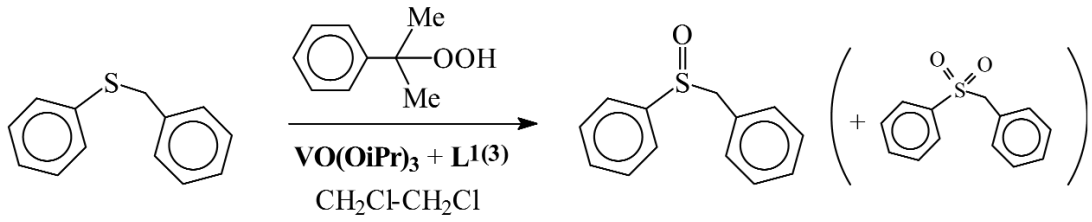

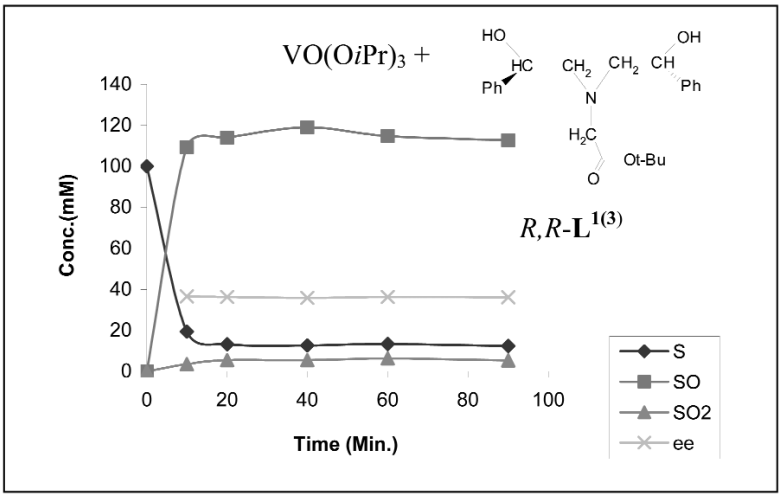

Fig. 4 Reaction scheme (top) and graphical presentation of the catalytically conducted reaction course. S = sulfide, SO = sulfoxide, SO2 = sulfone, ee = enantiomeric excess. The catalyst [$VO(OiPr)_3$ + *R,R*-$\mathbf{L^{1(3)}}$] concentration is 10 mM, *c*(sulfide) and *c*(peroxide) are ca. 100 mM. Solvent: CH_2ClCH_2Cl, T = 251 K.

THE PEROXO COMPLEX

Reaction of aqueous potassium vanadate, 2,5-dipicolinic acid ($H_2\mathbf{L^2}$) and H_2O_2 yielded red crystals of $K_3[VO(O_2)(\mathbf{L^2})_2]\cdot 4.5H_2O$, $K_3\mathbf{3}\cdot 4.5H_2O$ (see Fig. 5 for an ORTEP plot, and Table 2 for structure parameters of the anion **3**). For selected IR data, see Table 1; the chemical shift $\delta(^{51}V)$ in D_2O is –623 ppm. The anion **3** shows the pentagonal–bipyramidal structure common of peroxovanadium complexes [21]. The doubly bonded oxygen (O1) and one of the carboxylate oxygens (O6) form the axis. The carboxylate oxygens, O1 and O10/O11, are in bonding contacts with the potassium ion, the coordination sphere of which additionally contains 1–3 aqua ligands. K^+ is asymmetrically coordinated to the peroxo ligand (e.g., 2.799 and 2.938 for K2-O10/O11, and 2.831 and 3.203 Å for K1-O21/O22), which fact may be considered to mimic the hydroperoxo situation of the hydroperoxo intermediate postulated in the catalytic turnover (Fig. 2, vide supra). Possibly as a consequence of this bonding interaction, the η^2-bonded peroxo ligand (O10/O11) is slightly but significantly asymmetrically coordinated to the vanadium center. The *d*(O10-O11) is slightly shorter, the O10-V-O11 angle is slightly narrower than commonly observed in peroxovanadium complexes [22]. $K^+\cdots(O_2)V$ interaction has been described previously; no influence on the symmetrical side-on coordination of the peroxo group has, however, been observed [23]. In addition, there are intermolecular contacts between the anions mediated by π-π stacking (3.3 Å).

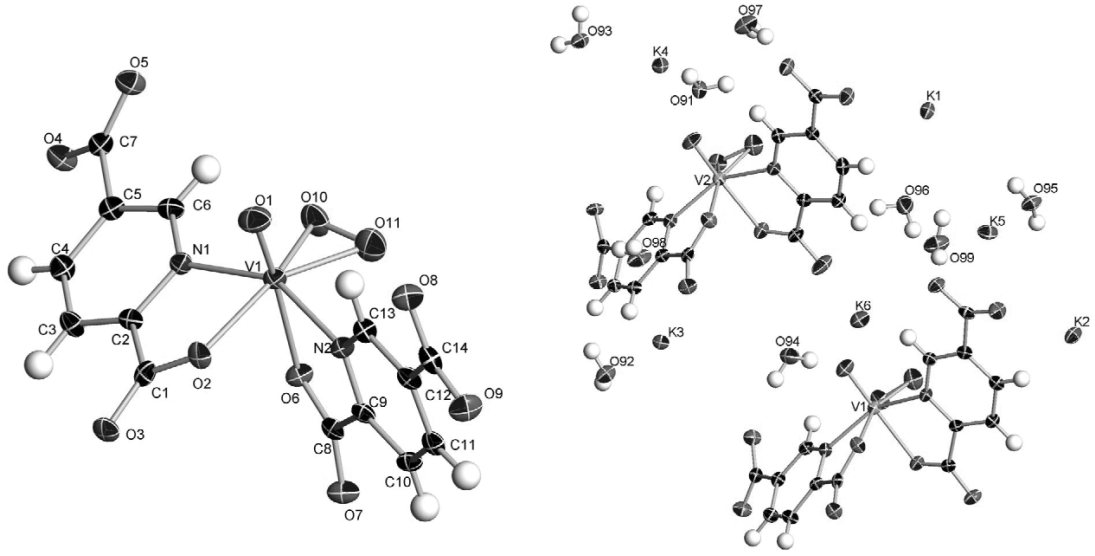

Fig. 5 ORTEP plot and numbering scheme for one of the two independent anions **3**, and an overview of the arrangement of the anions, the potassium counterions and the water molecules in K_3**3**·4.5H_2O.

COMPLEXES WITH SCHIFF BASES CONTAINING TYR AND SER CONSTITUENTS

Scheme 2 summarizes the reactions leading to the complexes [VO(naph-L-tyr)(H_2O)]·MeOH **4a**·MeOH (nap is the 2-oxonaphthaldehyde(1) moiety), [VO(van-D,L-tyr)(H_2O)]·H_2O **4b**·H_2O (van = *o*-vanillin) and [VO(van-D,L-ser)(H_2O)]·2H_2O **5**·2H_2O. For IR characteristics, see Table 1. ORTEP plots of **4b** and **5** are shown in Fig. 3, selected structure parameters for **4b** and **5** are listed in Table 2. The structure parameters for **4a** ([VO(naph-L-Tyr)(H_2O)] are about the same as for the previously reported [VO(naph-D-Tyr)(H_2O)] [24]. The compounds were prepared from vanadyl sulfate and the Schiff-base precursors, or from the VO-bis(aldehydo) complexes and amino acids in acetate buffered water/ethanol under strict exclusion of air to yield the VO^{2+} complexes, i.e., in analogy to [VO(nap-D-tyr)(H_2O)] [24]. In the presence of oxygen, VO^{3+} or mixed VO^{2+}/VO^{3+} complexes can form. Examples are the dinuclear, oxo-bridged serine Schiff-base complexes [{VO(van-L-ser)(H_2O)}$_2\mu$-O] [25] and [{VO(sal-D,L-ser)}$_2\mu$-O]$^-$ (sal = salicylaldehyde) [26]. The formation of complexes **4b** and **5** is accompanied by racemization of the amino acid constituent.

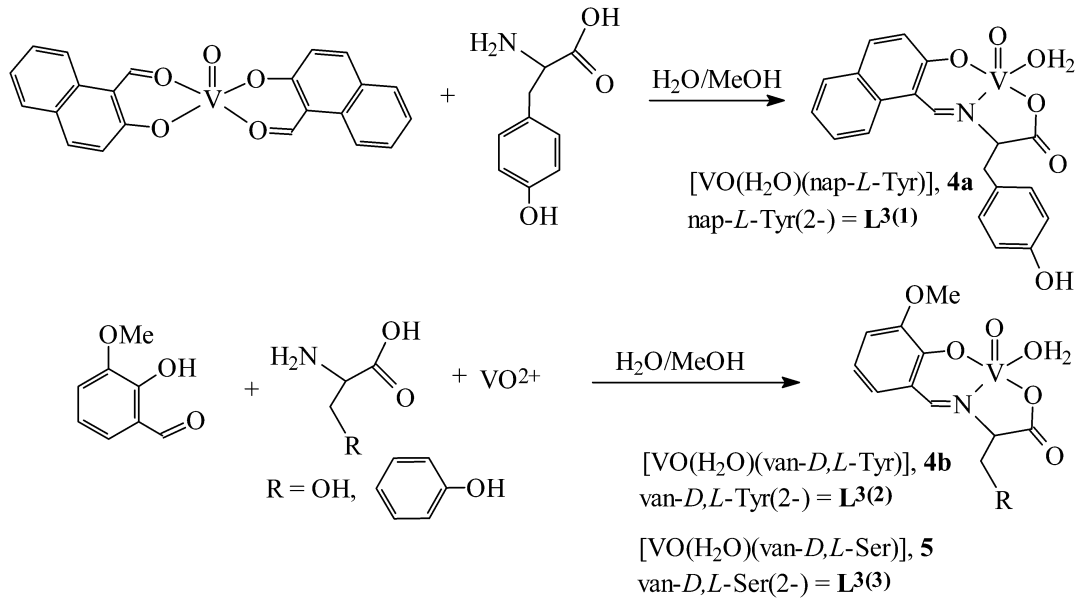

Scheme 2

All of the bonding parameters are in the expected range. The complexes show only minimal distortions from the square pyramid (τ values are close to 0.1). Vanadium is above the plane formed by three ligand functions and H_2O by 0.58–0.60 Å. The coordinated water and the water/methanol of crystallization, the carboxylate oxygens, the dangling OH of the Tyr and Ser moieties, and, in the case of **4b** and **5**, also the oxo group on V and the methoxy group of vanillin are involved in complex hydrogen-bonding networks, features which model the embedment of the vanadate centers in the proteins. Sections of these inter- and intramolecular networks are depicted in Scheme 3.

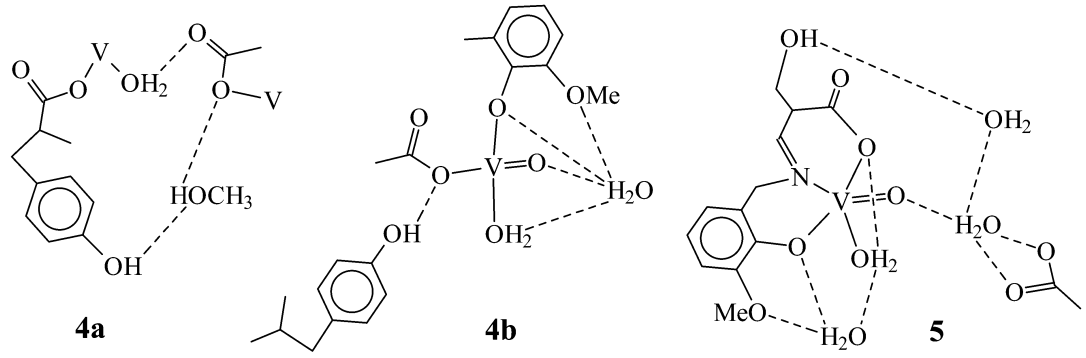

Scheme 3

Electron paramagnetic resonance (EPR) data (Table 3) unequivocally show that the solid-state arrangement is retained in solution. The A_z components of the hyper-fine coupling constants are in accord with an equatorial ligand set constituting water, phenolate-O, carboxylate-O, and imine-N [27].

Table 3 EPR data for compounds **4** and **5**.

	A_{iso}	g_{iso}	A_{xy}	A_z	g_{xy}	g_z
4b	93	1.991	61	170	1.982	1.951
5	91.3	1.9877	62	171	1.982	1.949

CONCLUSION

Oxovanadium compounds have been structurally characterized, which model the catalytic centers of VPOs and vanadate-inhibited acid phosphatases (acid ViPs). The V^V compounds **1** and **2** contain an O_4N donor set in an essentially trigonal–bipyramidal environment, with the oxo group in the plane, and the axial positions occupied by OMe (corresponding to the axial OH in the cofactor) and nitrogen (represented by an amine-N and corresponding to the axial His in VPO and acid ViP). The chirality of the protein pocket is mimicked by chiral centers in the ligand periphery of the complexes. The in situ generated complex **1** (and **2**, as well as authentic **1** and **2**; not shown) mimic the sulfideperoxidase activity of the VPO. The anionic oxo-peroxo complex **3** contains a slightly asymmetrically side-on coordinated peroxo ligand, due to bonding interactions of one of the peroxo oxygens with the potassium counterion, reminiscent of the hydroperoxo intermediate proposed as the site of substrate attack in catalytic turnover. The oxovanadium(IV) complexes **4** and **5** have tetragonal geometry and resemble the inactive, reduced (V^{IV}) state of the peroxidases. These complexes had been designed to model axial serine and tyrosine coordination in vanadate-inhibited alkaline phosphatases; the Ser-OH and Tyr-OH remain, however, dangling due to preferential coordination of the terminal carboxylato group. The V···O(Ser) distance in **5**, 4.39 Å, and the involvement of the Ser-OH in hydrogen-bonding models corresponding features in the active site of the VPOs.

Deposition of crystal data: 1: CCDC-246157, **2:** CCDC-246616, K_3**3**·4.5H_2O: CCDC-244107, **4a**·MeOH: CCDC-235864, **4b**·H_2O: CCDC-235866, **5**·2H_2O: CCDC-235867.

ACKNOWLEDGMENT

This work was supported by the Deutsche Forschungsgemeinschaft.

REFERENCES

1. (a) H. B. ten Brink, A. Tuynman, H. L. Dekker, W. Hemrika, Y. Izumi, T. Oshiro, H. E. Schoemaker, R. Wever. *Inorg. Chem.* **37**, 6780 (1998); (b) H. B. ten Brink, H. L. Holland, H. E. Schoemaker, H. van Lingen, R. Wever. *Tetrahedron: Asymmetry* **10**, 4563 (1999).
2. M. Weyand, H.-J. Hecht, M. Kieß, M.-F. Liaud, H. Vilter, D. Schomburg. *J. Mol. Biol.* **293**, 595–611 (1999).
3. (a) M. I. Isupov, A. R. Dalby, A. A. Brindley, Y. Izumi, T. Tanabe, G. N. Murshudov, J. A. Littlechild. *J. Mol. Biol.* **299**, 1035–1049 (2000); J. A. Littlechild and E. Gorcia-Rodriguez. *Coord. Chem. Rev.* **237**, 65–76 (2003).
4. (a) A. Messerschmidt and R. Wever. *Proc. Natl. Acad. Sci. USA* **93**, 392–396 (1996); (b) S. Macedo-Ribeiro, W. Hemrika, R. Renirie, R. Wever, A. Messerschmidt. *J. Biol. Inorg. Chem.* **4**, 209 (1999); (c) N. Tanaka, Z. Hasan, R. Wever. *Inorg. Chim. Acta* **356**, 288–296 (2003).
5. A. Messerschmidt, L. Prade, R. Wever. *Biol. Chem.* **378**, 309–315 (1997).
6. (a) K. Ishikawa, Y. Mihara, K. Gondoh, E. Susuki, Y. Asano. *EMBO J.* **19**, 2412–2423 (2000); (b) Y. Lindqvist, G. Schneider, P. Vihko. *Eur. J. Biochem.* **221**, 139–142 (1994).
7. K. M. Holtz, B. Stec, E. R. Kantrowitz. *J. Biol. Chem.* **274**, 8351–8354 (1999).
8. M. Zhang, M. Zhou, R. L. Van Etten, C. V. Stauffacher. *Biochemistry* **36**, 15–23 (1997).

9. W. Hemrika, R. Renirie, H. L. Dekker, P. Barnett, R. Wever. *Proc. Natl. Acad. Sci. USA* **94**, 2145–2149 (1997).
10. N. Tanaka, V. Dumay, Q. Liao, A. J. Lange, R. Wever. *Eur. J. Biochem.* **269**, 2162–2167 (2002).
11. R. Renirie, W. Hemrika, R. Wever. *J. Biol. Chem.* **275**, 11650–11657 (2000).
12. (a) A. Butler. *Coord. Chem. Rev.* **187**, 17–25 (1999); (b) B. J. Hamstra, G. J. Colpas, V. L. Pecorao. *Inorg. Chem.* **37**, 949–955 (1998); (c) M. Časný, D. Rehder, H. Schmidt, H. Vilter, V. Conte. *J. Inorg. Biochem.* **80**, 157–160 (2000).
13. O. Bortolini, M. Carrano, V. Conte, S. Moro. *Eur. J. Inorg. Chem.* 42–46 (2003).
14. (a) J. M. Arber, E. deBoer, C. D. Garner, S. S. Hasnain, R. Wever. *Biochemistry* **28**, 7968–7973 (1989); (b) E. deBoer, K. Boon, R. Wever. *Biochemistry* **27**, 1629 (1988).
15. (a) N. D. Chasteen. *Struct. Bonding (Berlin)* **53**, 105 (1983); (b) M. J. Gresser, A. S. Tracey, P. Stankiewicz. *J. Adv. Protein Phosphatases* **4**, 35 (1987); (c) N. D. Chasteen. In *Metal Ions in Biological Systems*, Vol. 31, Chap. 7, H. Sigel and A. Sigel (Eds.), Marcel Dekker (1995); (d) H. Sun, M. C. Cox, H. Li, P. Sadler. *Struct. Bonding* **88**, 71 (1997); (e) P. J. Stankiewicz, A. S. Tracey, D. C. Crans. In *Metal Ions in Biological Systems*, Vol. 31, Chap. 9, H. Sigel and A. Sigel (Eds.), Marcel Dekker (1995).
16. (a) G. L. Mendz. *Arch. Biochem. Biophys.* **291**, 201–211 (1991); (b) P. J. Stankiewicz, M. J. Gresser, A. S. Tracey, L. F. Hass. *Biochemistry* **26**, 629–638 (1987).
17. D. C. Crans and C. M. Simone. *Biochemistry* **30**, 6734–6741 (1991).
18. A. W. Addison, T. N. Rao, J. Reedijk, J. van Rijn, G. C. Verschoor. *J. Chem. Soc., Dalton Trans.* 1349–1356 (1984).
19. G. Santoni, G. M. Licini, D. Rehder. *Chem. Eur. J.* **9**, 4700–4708 (2003).
20. (a) K. Nakajima, M. Kojima, K. Kojima, J. Fujita. *Bull. Chem. Soc. Jpn.* **63**, 2620–2630 (1990); (b) C. Bolm and F. Bienewald. *Angew. Chem., Int. Engl.* **34**, 2640–2642 (1996).
21. (a) C. Bolm, G. Schlingloff, F. Bienewald. *J. Mol. Catal. A: Chem.* **117**, 347 (1997); (b) C. Bolm and F. Bienewald. *Synlett* **34**, 1327 (1998); (c) B. Pelotier, M. S. Anson, I. B. Campbell, S. J. F. Macdonald, G. Priem, R. F. W. Jackson. *Synlett* 1055 (2002).
22. M. Časný and D. Rehder. *Dalton Trans.* 839–846 (2004), and refs. cited therein.
23. M. Sivák, M Mad'arová, J. Tatiersky, J. Marek. *Eur. J. Inorg. Chem.* 2075–2081 (2003).
24. M. Ebel and D. Rehder. *Inorg. Chim. Acta* **356**, 210–214 (2003).
25. (a) C. Grüning and D. Rehder. *J. Inorg. Biochem.* **80**, 185–189 (2000); (b) C. Grüning, H. Schmidt, D. Rehder. *Inorg. Chem. Commun.* **2**, 57–59 (1999).
26. J. Costa Pessoa, J. A. L. Silva, A. L. Vieira, L. Vilas-Boas, P. O'Brien, P. Thornton. *J. Chem. Soc., Dalton Trans.* 1745 (1992).
27. (a) T. S. Smith II, R. LoBrutto, V. L. Pecoraro. *Coord. Chem. Rev.* **228**, 1–18 (2002); (b) A. J. Tasiopoulos, A. N. Troganis, A. Avangelou, C. P. Raptopoulou, A. Terzis, Y. Deligiannakis, T. A. Kabanos. *Chem. Eur. J.* **5**, 910–921 (1999).